





# The phenotypic and genotypic spectrum of individuals with mono- or biallelic ANK3 variants

Francesca Furia<sup>1,2</sup> | Amanda M. Levy<sup>3</sup> | Miel Theunis<sup>4</sup> | Michael J. Bamshad<sup>5,6,7</sup> |  
 Meghan N. Bartos<sup>8</sup> | Emilia K. Bijlsma<sup>9</sup> | Francesco Brancati<sup>10,11</sup> |  
 Lucile Cejudo<sup>12</sup> | Jessica X. Chong<sup>5,6</sup>  | Chiara De Luca<sup>10</sup> | Sarah Joy Dean<sup>8</sup> |  
 Alena Egense<sup>13</sup> | Himanshu Goel<sup>14,15</sup> | Adam J. Guenzel<sup>16</sup> | Ulrike Hüffmeier<sup>17</sup> |  
 Eric Legius<sup>4</sup> | Grazia M. S. Mancini<sup>18,19</sup> | Iñigo Marcos-Alcalde<sup>20</sup> |  
 Tanguy Niclass<sup>12</sup> | Marc Planes<sup>21</sup> | Sylvia Redon<sup>22,23</sup> | David Ros-Pardo<sup>20</sup>  |  
 Karen Rouault<sup>22,23</sup> | Rachel Schot<sup>18,24</sup> | Sarah Schuhmann<sup>17</sup> | Joseph J. Shen<sup>13</sup> |  
 Alice M. Tao<sup>25</sup> | Isabelle Thiffault<sup>26,27</sup> | Hilde Van Esch<sup>4,28</sup> |  
 Ingrid M. Wentzensen<sup>16</sup> | Tahsin Stefan Barakat<sup>18,19,24</sup>  | Rikke S. Møller<sup>1,2</sup> |  
 Paulino Gomez-Puertas<sup>20</sup> | Wendy K. Chung<sup>29,30</sup> | Elena Gardella<sup>1,2,31</sup> |  
 Zeynep Tümer<sup>3,32</sup> 

## Correspondence

Zeynep Tümer and Amanda M. Levy,  
 Department of Clinical Genetics, Kennedy  
 Center, Copenhagen University Hospital,  
 Rigshospitalet, Copenhagen, Denmark.  
 Email: [zeynep.tumer@regionh.dk](mailto:zeynep.tumer@regionh.dk) and [marie.amanda.bust.levy@regionh.dk](mailto:marie.amanda.bust.levy@regionh.dk)

## Funding information

NHGRI, Grant/Award Numbers: U01  
 HG011744, U24 HG011746; Netherlands  
 Organisation for Scientific Research,  
 Grant/Award Number: 09150172110002;  
 Italian Ministry of Health; Italian Ministry of  
 University and Research, Grant/Award  
 Numbers: PRIN2022, PRIN PNRR 2022;  
 P50HD109879; Spanish Government,  
 Grant/Award Numbers: RTI2018-094434-B-  
 I00, PID2021-126625OB-I00

## Abstract

ANK3 encodes ankyrin-G, a protein involved in neuronal development and signaling. Alternative splicing gives rise to three ankyrin-G isoforms comprising different domains with distinct expression patterns. Mono- or biallelic ANK3 variants are associated with non-specific syndromic intellectual disability in 14 individuals (seven with monoallelic and seven with biallelic variants). In this study, we describe the clinical features of 13 additional individuals and review the data on a total of 27 individuals (16 individuals with monoallelic and 11 with biallelic ANK3 variants) and demonstrate that the phenotype for biallelic variants is more severe. The phenotypic features include language delay (92%), autism spectrum disorder (76%), intellectual disability (78%), hypotonia (65%), motor delay (68%), attention deficit disorder (ADD) or attention deficit hyperactivity disorder (ADHD) (57%), sleep disturbances (50%), aggressivity/self-injury (37.5%), and epilepsy (35%). A notable phenotypic difference was presence of ataxia in three individuals with biallelic variants, but in none of the individuals with monoallelic variants. While the majority of the monoallelic variants are predicted to result in a truncated protein, biallelic variants are almost exclusively missense. Moreover, mono- and

Francesca Furia and Amanda M. Levy contributed equally.

For affiliations refer to page 9

This is an open access article under the terms of the [Creative Commons Attribution-NonCommercial-NoDerivs](https://creativecommons.org/licenses/by-nc-nd/4.0/) License, which permits use and distribution in any medium, provided the original work is properly cited, the use is non-commercial and no modifications or adaptations are made.

© 2024 The Author(s). *Clinical Genetics* published by John Wiley & Sons Ltd.

biallelic variants appear to be localized differently across the three different ankyrin-G isoforms, suggesting isoform-specific pathological mechanisms.

#### KEYWORDS

aggressivity, ankyrin-G, autism spectrum disorder, epilepsy, hypotonia, intellectual disability, language delay, neurodevelopmental disorder, sleep disturbances

## 1 | INTRODUCTION

Ankyrin-G (also known as ankyrin-3), encoded by *ANK3*, is a scaffolding protein important for neuronal organization, signaling, and brain development through its function as a linker between membrane proteins (e.g., sodium channels) and the cytoskeleton.<sup>1,2</sup> As a result of alternative splicing, ankyrin-G has three major isoforms: the widely expressed 190 kDa isoform and the 270 and 480 kDa isoforms, which are primarily expressed in the brain (Figure 1). All three isoforms share three functional domains. The N-terminal membrane-binding domain comprises 24 ankyrin repeats (ANKRs) and acts as a scaffold for numerous membrane proteins. These are indirectly linked to the actin/spectrin cytoskeleton by the spectrin-binding domain (SBD), which comprises one UPA and two ZU5 domains. The C-terminal regulatory domain, which includes a death domain and an unstructured domain, modulates interactions with the ANKRs and SBD.<sup>1,3-5</sup> The two larger 270 and 480 kDa isoforms have an additional giant exon domain, resulting from partial or full utilization of a 7.8 kb exon (Figure 1A, B), respectively. This domain localizes these isoforms to the axon initial segments and Ranvier's nodes, where they act as master organizers.<sup>1</sup> In mouse brain, the three isoforms differ in their temporal expression. The expression of the 480 kDa isoform peaks at birth and decreases until stabilizing at adolescence. In contrast, expression of the 190 kDa isoform increases from birth and stabilizes from adolescence into adulthood, while the 270 kDa isoform is consistently expressed throughout life.<sup>5</sup>

Mono- and biallelic *ANK3* variants have been reported in 14 individuals with features including intellectual disability (ID), speech impairment, autism spectrum disorder (ASD), attention deficit hyperactivity disorder (ADHD), ataxia, and epilepsy.<sup>6-12</sup> Furthermore, 10 *ANK3* variants (three biallelic and seven monoallelic) have been identified through genomic sequencing of individuals with either ASD<sup>13-15</sup> or ID and epilepsy,<sup>16-19</sup> but the clinical information was limited. Here, we describe 13 previously unreported individuals with mono- or biallelic *ANK3* variants and review the 14 previously published individuals with detailed clinical information to improve our understanding of the correlation of *ANK3* associated clinical features.

## 2 | MATERIALS AND METHODS

### 2.1 | Collection of clinical data

The unpublished individuals with either mono- or biallelic *ANK3* variants were recruited from international genetic centers through

Matchmaker Exchange.<sup>20</sup> The parents or legal guardians of all probands have provided written informed consent. The study was approved by local ethical committees. The authors of the studies describing the previously published individuals were contacted, but no new data were available.

### 2.2 | Identification and evaluation of *ANK3* variants

*ANK3* variants were identified through clinical exome or genome sequencing. The variants have been annotated using the *ANK3* transcript NM\_020987.5 (GRCh38/hg38) coding for the 480 kDa isoform and described using the HGVS (Human Genome Variation Society) nomenclature recommendations (<https://varnomen.hgvs.org/>). The presence of *ANK3* variants in control populations was reviewed using the Genome Aggregation Database (gnomAD v4.0.0, accessed November 3rd 2023; <https://gnomad.broadinstitute.org/>), and the pathogenicity of each variant was assessed according to ACMG/AMP (American College of Medical Genetics and Genomics/Association for Molecular Pathology) criteria.<sup>21</sup> The SpliceAI tool (<https://github.com/Illumina/SpliceAI>) was employed to predict the missense variants' effect on splicing, and the NMDescPredictor tool (<https://nmdprediction.shinyapps.io/nmdescpredictor/>) was used to assess the ability of the protein truncating variants (PTVs) to escape nonsense-mediated decay (NMD). CADD (combined annotation dependent depletion, <https://cadd.gs.washington.edu/>) scores were used to evaluate the predicted deleteriousness of all variants. All individuals with missense variants with CADD scores below 20 were excluded from the study.

### 2.3 | Structural modeling and molecular dynamics simulation of *ANK3* missense variants

The 3D structures of the ANKR domain (ANKRD), SBD, and death domain of wild-type (WT) ankyrin-G (UniprotKB id: Q12955) were modeled using the crystal structures of ankyrin-B repeats domain (PDB ID: 4RLV)<sup>22</sup> and SBD-death tandem (PDB ID: 4D8O)<sup>23</sup> as templates. Due to unstructured sequences and the lack of a suitable template, it was not possible to generate a structural model of sufficient quality for the remaining domains. Domain structures with the *ANK3* missense variants were modeled using the reference sequence as a template and molecular dynamics simulation was performed as described previously<sup>24</sup> (Supplementary methods – Data S1).

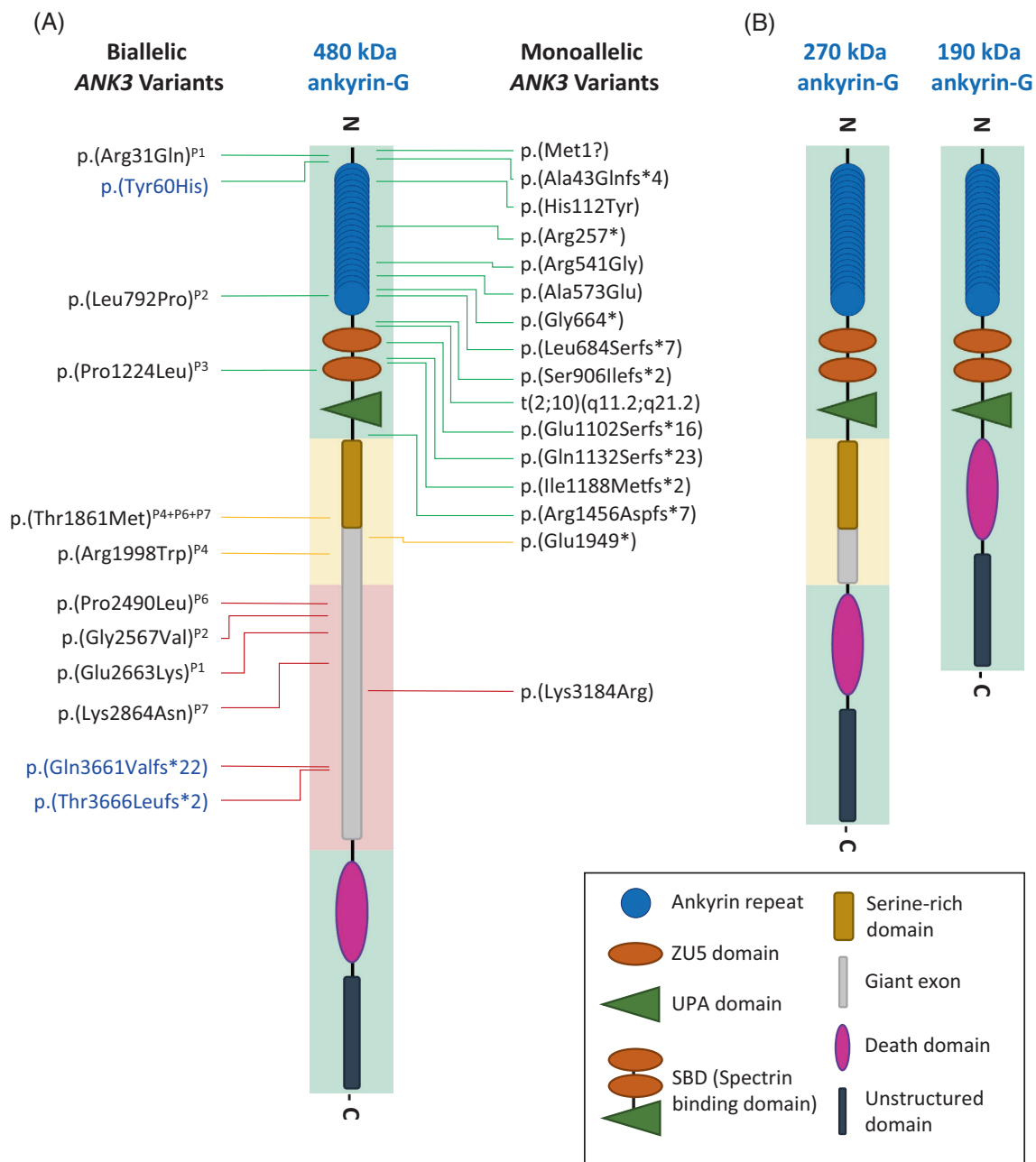


**FIGURE 1** Schematic overview of the ankyrin-G isoforms and variants. The color of the protein background bar and the lines indicating variant position illustrate whether a region and variant is present in all three protein isoforms (green), the 270 and 480 kDa isoforms (yellow), or solely the 480 kDa isoform (red). The ankyrin repeats comprise the membrane-binding region, the ZU5 and UPA domains comprise the spectrin-binding domain, and the regulatory region comprise the death domain and the unstructured C-terminal region, with or without the serine-rich domain and the giant exon. (A) The 480 kDa ankyrin-G isoform (NM\_020987.5) as well as the position of the biallelic (left) and monoallelic (right) ANK3 variants. The microdeletion is not included. Compound heterozygous variants are *in trans* with the variant with the same proband number in superscript. Homozygous variants are in blue. (B) The 270 kDa (left) and 190 kDa (right) isoforms. [Colour figure can be viewed at [wileyonlinelibrary.com](https://onlinelibrary.wiley.com)]

### 3 | RESULTS

The clinical and genetic data of 14 previously published and 13 newly identified individuals with mono- or biallelic ANK3 variants are summarized in Tables 1 and 2 (see also Tables S1 and S2). Furthermore, data on two individuals with low CADD scores are presented in Table S1. Ten

individuals identified through cohort-studies are not included in the results and discussion section due to limited clinical information,<sup>13–19</sup> and their ANK3 variants are in Table S2. The frequencies of the main clinical features are calculated across the entire cohort and individuals are grouped according to whether they have biallelic ( $n = 11$ ) or monoallelic variants ( $n = 16$ ) to investigate a genotype–phenotype correlation (Table 1).

**TABLE 1** Clinical data in 27 individuals with bi- and monoallelic ANK3 variants.

Feature	Total cohort (n = 27)	Individuals with biallelic variants (n = 11)	Individuals with monoallelic variants (n = 16)
ID	78% (21/27)	91% (10/11)	69% (11/16)
Mild	33% (7/21)	20% (2/10)	46% (5/11)
Moderate	19% (4/21)	30% (3/10)	9% (1/11)
Severe	24% (5/21)	40% (4/10)	9% (1/11)
Unspecified	24% (5/21)	10% (1/10)	36% (4/11)
Language delay	92% (24/26)	100% (10/10)	87.5% (14/16)
Motor delay	68% (15/22)	86% (6/7)	60% (9/15)
Behavioral and/or psychiatric disturbances	100% (26/26)	100% (10/10)	100% (16/16)
Epilepsy	35% (9/26)	50% (5/10)	25% (4/16)
Sleep disorders	50% (10/20)	71% (5/7)	38% (5/13)
Hypotonia	65% (15/23)	78% (7/9)	57% (8/14)
Ataxia	20% (3/15)	50% (3/6)	0% (0/9)
Cerebral imaging abnormalities	45% (9/20)	45% (5/11)	44% (4/9)

Abbreviations: ASD, autistic spectrum disorder; ID, intellectual disability; n, number.

### 3.1 | Phenotypic spectrum

The cohort comprised 27 individuals from 25 families (14 males and 13 females). The median age at the last examination was 8 years (from 18 months to 34 years). All individuals, except three previously published siblings (Family I, P9-11),<sup>10</sup> were unrelated. Detailed clinical information can be found in Table 1 and Table S1. Most individuals (55%, 12/22) were born at term following an unremarkable pregnancy.

Motor delay was reported in 68% (15/22), while language was delayed in 92% (24/26). Through clinical evaluation, ID was observed in 21 out of 27 individuals (78%) old enough to be evaluated: seven with mild (33%), four with moderate (19%), and five with severe ID (24%). In five individuals, ID severity was not specified (24%). Three individuals were borderline, and one was reported with learning disability. Two individuals were reported to have normal cognition (P14 and P27).

Behavioral and psychiatric disturbances were common (26/26, 100%) and included autistic features (16/21, 76%), ADHD/ADD (12/21, 57%), aggressive/self-injurious behavior (9/24, 38%), and anxiety (5/24, 21%). Ataxia was reported in 3/15 (20%) and hypotonia in 15/23 (65%) individuals and in two of them only in childhood.

Nine out of 26 individuals (35%) had seizures with median onset at 6 months of age (ranging from 4 months to 12 years). Epilepsy phenotype was described in detail for only two patients. The most common seizure types were epileptic spasms, absence-like seizures, febrile seizures, myoclonic seizures, and generalized tonic-clonic seizures. Different sleep disturbances were described in 10/20 individuals (50%) (Table S1).

Nonspecific dysmorphic features were observed in 13/22 (59%) of individuals, and few individuals had vision disorders such as strabismus and or myopia. Brain neuroimaging (magnetic resonance or computerized tomography) was performed in 20 individuals, and nine of

them (42%) had non-specific abnormalities, such as corpus callosum hypoplasia in three, white matter hyperintensities in three, and cerebellar vermis hypoplasia in two individuals (Table S1).

### 3.2 | Molecular spectrum of ANK3 variants

Among the 27 individuals with detailed clinical information, 29 unique mono- or biallelic ANK3 variants (16 novel) were detected (Table 2). Monoallelic variants were identified in 16 individuals, of which four were missense and 12 were PTVs comprising one start-loss, three nonsense and seven frameshift variants, and one balanced translocation with one of the breakpoints in intron 25 of ANK3 (P25).<sup>10</sup> Five homozygous and six compound heterozygous variants were found in 11 individuals, all unrelated except from a sibling trio.<sup>10</sup> These biallelic variants were missense/missense, except two homozygous frameshift variants p.(Thr3666Leufs\*2) and p.(Gln3661Valfs\*22) and one microdeletion *in trans* with a missense variant (P3). Only a single variant p.(Thr1861Met) was observed three times in unrelated biallelic individuals (P4, P6, and P7).<sup>9</sup> Segregation data were available for 12 heterozygous individuals and the variants occurred *de novo* in all except for P27, where one of the parents showed 22% mosaicism in blood<sup>12</sup> (Tables S1 and S2). All individuals with biallelic variants except one (P3) for whom segregation data were available had inherited the variants from their respective parents. None of the parents were reported to be clinically affected, except the father of P1 (missense/missense) who had epilepsy and the mother of P3 (missense/copy number variant) who had ADHD. P3 was compound heterozygous for a maternally inherited missense variant and a *de novo* microdeletion encompassing 25 protein-coding genes, six of which were OMIM morbid genes (ANK3, PCDH15, TFAM, BICC1, ZNF365, and EGR2; DECIPHER GRCh38, [www.deciphergenomics.org](http://www.deciphergenomics.org)). Of these genes PCDH15 and TFAM are associated with autosomal recessive and/or

**TABLE 2** Mono- and biallelic ANK3 variants in 27 individuals from 25 families.

Ind	Fam	Zygoty	Allele 1			Allele 2			Ref.
			Coding effect	Variant description	CADD score	Coding effect	Variant description	CADD score	
P1	A	Comp het	Mis	c.92G>A	26	Mis	c.7987G>A	22	Present
P2	B	Comp het	Mis	c.2375T>C	28	Mis	c.7700G>T	23	Present
P3	C	Comp het	Mis	c.3671C>T	28	CNV	g.54287239_63861376del	NA	Present
P4	D	Comp het	Mis	c.5582C>T	23	Mis	c.5992C>T	20	Present
P5	E	Hom	Mis	c.178T>C	25	Mis	c.178T>C	25	11
P6	F	Comp het	Mis	c.5582C>T	23	Mis	c.7469C>T	22	9
P7	G	Comp het	Mis	c.5582C>T	23	Mis	c.8592G>T	23	9
P8	H	Hom	Fs	c.10981_10982del	33	Fs	c.10981_10982del	33	6
P9	I	Hom	Fs	c.10995del	33	Fs	c.10995del	33	10
P10	I								
P11	I								
P12	J	Het	Start-loss	c.1A>G	24	NoV			Present
P13	K	Het	Mis	c.334C>T	28	NoV			Present
P14	L	Het	Mis	c.1621C>G	25	NoV			Present
P15	M	Het	Mis	c.1718C>A	28	NoV			Present
P16	N	Het	Fs	c.2716_2713dup	33	NoV			Present
P17	O	Het	Fs	c.3394del	22	NoV			Present
P18	P	Het	Fs	c.3564del	24	NoV			Present
P19	Q	Het	Fs	c.4365_4368del	32	NoV			Present
P20	R	Het	Mis	c.9551A>G	22	NoV			Present
P21	S	Het	Fs	c.127del	32	NoV			Present
P22	T	Het	Non	c.769C>T	38	NoV			8
P23	U	Het	Non	c.1990G>T	38	NoV			7
P24	V	Het	Fs	c.2050del	32	NoV			8

(Continues)

TABLE 2 (Continued)

Ind	Fam	Zygoty	Allele 1				Allele 2			
			Variant description	CADD score	Predicted protein	Coding effect	Variant description	CADD score	Predicted protein	Coding effect
P25	W	Het	t(2;10)(q11.2;q21.2)g.94761852_qterdelins [g.60116221_qter] g.60116221_qterdelins [g.93667845_qter]	NA	p.?	NoV				10
P26	X	Het	c.3303del	8	p.(Glu1102Serfs*16)	NoV				8
P27	Y	Het	c.5843_5844dup	33	p.(Glu1949*)	NoV				12

Note: Coding variants are described using transcript NM\_020987.5 and structural variants using NC\_000010.11. One group of variants is biallelic and the other group of variants is monoallelic. Abbreviations: comp het, compound heterozygous; del, deletion; fam, family; fs, frameshift; het, heterozygous; hom, homozygous; ind, individual; mis, missense; NA, not applicable; non, nonsense; ref, reference; CNV, copy number variant; Trans, translocation; NoV, no other variant detected.

digenic recessive conditions, and *BICC1* and *ZNF365* are susceptibility genes. *EGR2* is associated with autosomal recessive or autosomal dominant hypomyelinating neuropathy, and almost all the heterozygous variants reported in affected individuals are missense (Table S2).<sup>25</sup>

None of the PTVs were predicted to escape NMD, and missense variants were not predicted to affect splicing (Table S2). All the monoallelic variants were absent in control populations. The biallelic variants were either absent or present in very low frequency (<0.006%), except two variants (p.(Thr1861Met) and p.(Pro2490Leu)) which had an allele frequency of 0.431% and 0.044%, respectively (Table S2). Notably, both variants were shown to be pathogenic through functional studies.<sup>9</sup>

Using ACMG criteria, five of the biallelic variants were classified as variants of uncertain significance (VUS) and six were classified as likely pathogenic (LP) or pathogenic (P). Of the monoallelic variants, 15 variants are classified as LP/P and one as VUS (Table S2).

### 3.3 | Structural prediction of ankyrin-G variants

3D models of the reference and nine missense variants within the ANKRD and SBD-death domain of ankyrin-G were obtained through homology modeling and were then subjected to molecular dynamics simulation (Figure 2A, B). All functional domains universally present in all isoforms were modeled, except for the C-terminal unstructured domain. Obtaining a quality model of the latter, as well as of the isoform-specific giant exon and serine-rich domains was impeded due to unstructured sequences and the lack of suitable templates. The biallelic p.(Arg31Gln) is located in the interaction region between the N-terminal segment and the first ANKR domain and causes a conformational change in the protein by separating the N-terminal tail from the repeats (Figure 2C). Furthermore, the variant is *in trans* with p.(Glu2663Lys) (not modeled), and both residue substitutions change the side chain charges (positive to uncharged and negative to positive, respectively), which may affect local stability or potential interactions. p.(Arg541Gly) and p.(Ala573Glu), both monoallelic, are located near the ANKRD surface (Figure 2A) where they alter the surface electrostatic charge by disrupting the continuity of a positively charged patch or expanding a negatively charged patch, respectively (Figure 2D, E), possibly affecting interactions with other macromolecules. Moreover, as p.(Ala573Glu) is located between ANKRs, the change of the small alanine for the larger glutamate also distorts the relative repeat position, which may cause long-term destabilization of the domain. Pro1224 is, together with Pro1223 and Pro1225, part of a rigid loop which precedes an  $\alpha$ -helix (Figure 2F). The biallelic p.(Pro1224Leu) substitution, which is found *in trans* to a copy number variant, introduces flexibility to this region, greatly destabilizing the local structure of the second ZU5 domain and is predicted to cause the loss of the adjacent  $\alpha$ -helix (Figure 2F). Finally, the simulation for the homozygous p.(Tyr60His), the heterozygous p.(His112Tyr), and the compound heterozygous p.(Leu792Pro), which is *in trans* to p.(Gly2567Val) (not modeled), shows no significant effect on the structure or mobility of



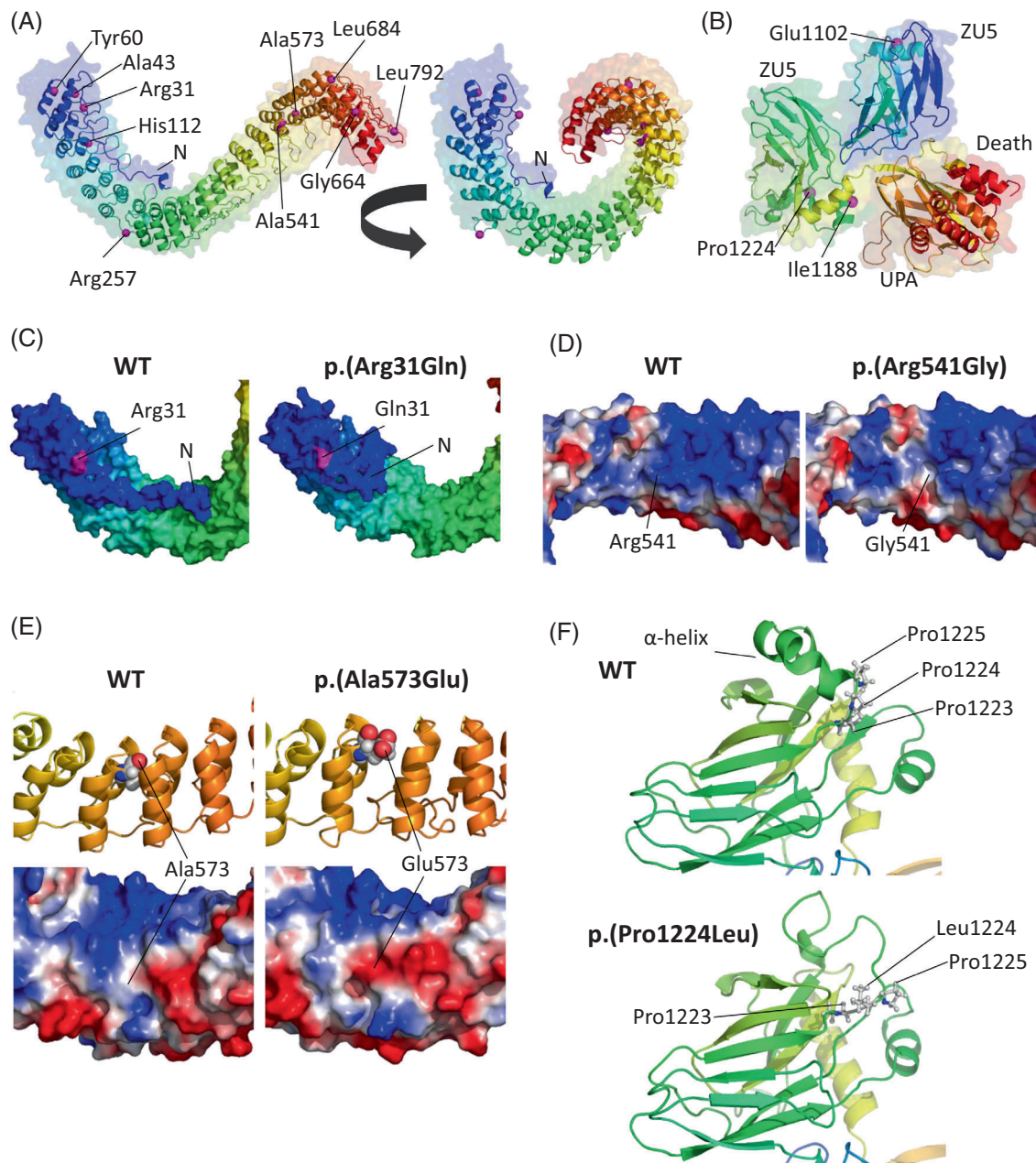


**FIGURE 2** Structural models of the ANK3 wild-type (WT) and variant domains. The WT ankyrin-repeat domain (ANKRD) (A) and spectrin-binding domain (SBD)-death motifs (B) with variant positions represented as pink spheres. (C) The p.(Arg31Gln) variant induces a conformational change affecting the position of the N-terminal (N). (D) p.(Arg541Gly) and (E) p.(Ala573Glu) alter the surface electrostatic charges. (F) p.(Pro1224Leu) destabilizes the local structure of the second ZU5 domain due to abnormal flexibility and the loss of an  $\alpha$ -helix. [Colour figure can be viewed at [wileyonlinelibrary.com](http://wileyonlinelibrary.com)]

the domain (Figure S1A–C), although an impaired domain folding process cannot be ruled out.

### 3.4 | Genotype–phenotype correlation

We compared the phenotypes of the individuals with biallelic variants to those who have monoallelic variants (Table 1). A notable

observation was the presence of ataxia in three individuals (3/6) with biallelic variants, while it was not reported in individuals with monoallelic individuals (0/9). Furthermore, motor and language delay, ID, aggressive self-injurious behavior, ASD, ADHD/ADD, hypotonia, sleep disturbances, and epilepsy were observed more often in individuals with biallelic variants compared to those with monoallelic individuals. Anxiety was reported only in individuals with monoallelic variants (5/16).

## 4 | DISCUSSION

In this study we describe the clinical features and genotypes of 27 (13 new and 14 published) individuals with mono- or biallelic ANK3 variants, corroborating the ANK3-related neurodevelopmental disorder as a disease primarily affecting brain function. As the different isoforms of ankyrin-G play distinct and important roles in neuronal development and signaling, a defective protein would be expected to lead to a wide array of neurological manifestations. Indeed, the main clinical manifestations in the reported individuals are language delay (92%), behavioral/psychiatric features (100%), ID (78%), motor delay (68%), hypotonia (65%), sleep disturbances (50%), and epilepsy (35%). The most common behavioral/psychiatric features were ASD (76%), ADHD/ADD (57%), and aggressive self-injurious behavior (38%).

In general, individuals with biallelic variants had more clinical features compared to those with monoallelic variants. Similar correlations have been made for the developmental epileptic encephalopathies related to variants in *SCN8A*, encoding the pore-forming subunit in the voltage gated sodium channel  $\text{Na}_v1.6$ ,<sup>26</sup> and *GRIN2A*, which encodes a glutamatergic NMDA receptor subunit.<sup>27</sup> When comparing the phenotypes, a notable observation was the presence of ataxia in three individuals with biallelic variants (3/6), but none of the individuals with monoallelic variants (0/9) had this feature. On the other hand, anxiety was only observed in individuals with monoallelic variants. However, we have not identified a clear phenotype-genotype correlation, and the number of individuals is too small to associate ataxia with biallelic and anxiety with monoallelic variants.

Variants in *ANK3* have repeatedly been linked to schizophrenia and bipolar disorder<sup>5</sup> and increased anxiety was observed in heterozygous *Ank3* knockout mice.<sup>28</sup> In the present cohort, we observe a high frequency of behavioral disturbances, especially aggressive behavior, and anxiety has been reported in five of the individuals with monoallelic variants. Bipolar disorder or schizophrenia has not been observed in any individuals in this cohort, but this may be due to the young age at the last examination.

*ANK3* has a LOEUF (loss-of-function observed/expected upper bound fraction) value of 0.12, suggesting that it is intolerant to loss-of-function variants, and similarly, a Z-score of 5.35 which indicates that the gene is also intolerant to missense variants (gnomAD database). When considering the variant localization, it is notable that we have not detected any variants in the C-terminus of the protein, namely the death domain and the unstructured domain. In contrast, most of the monoallelic variants (14/16) are in the N-terminus of the protein within two domains, ANKRD and SBD, which are present in all isoforms (Figure 1). Eleven of these variants are PTV, suggesting haploinsufficiency of all the isoforms as the disease mechanism for monoallelic variants. As most of the monoallelic variants are present in all three isoforms, we cannot exclude the presence of a second, for example, non-coding, variant *in trans* to the two monoallelic variants affecting only the larger isoforms (p.(Glu1949\*) and p.(Lys3184Arg)). Similarly, we cannot exclude the presence of a trans variant for the

three monoallelic missense variants p.(His112Tyr), p.(Arg541Gly), and p.(Ala573Glu). Unlike the monoallelic variants, the biallelic variants are not clustered. Putting the microdeletion aside, four of the 12 biallelic variants affect all the three isoforms, while two variants affect both the 270 and 480 kDa isoforms and six variants affect only the 480 kDa isoform. The only PTVs identified in a biallelic configuration (homozygous variants p.(Gln3661Valfs\*22) in P8 and p.(Thr3666Leufs\*2) in family I) are in the C-terminal of the giant exon which is present only in the 480 kDa isoform and thereby affect only this isoform (Figure 1). This suggests that biallelic PTVs within the domains common to all the isoforms or common to the 480 and the 270 kDa isoforms (serine-rich domain and the N-terminal of the giant exon) are not tolerated, while monoallelic PTVs in the giant exon are (supported by the presence of 57 monoallelic PTVs in gnomAD). Correspondingly, most of the biallelic variants are missense (10/12), suggesting that these variants may be hypomorphic, and may be detrimental when both alleles are affected and surpass a threshold. Further studies are necessary to understand the nature of the variants and their impact on disease phenotypes of heterozygotes for the missense variants. Mono- and biallelic variants are distributed differently, where monoallelic variants, mainly PTVs, are clustered in ANKRD and SBD, while most of the biallelic variants are in the giant exon domain. This may suggest that (1) variants exclusively affecting the larger isoforms are primarily deleterious when biallelic and (2) haploinsufficiency as a pathogenic mechanism mainly applies to the N-terminal domains shared by all three isoforms. This may be explained by the crucial role these domains play in the scaffolding-ability of ankyrin-G. The ANKRD binds, recruits, and organizes many transmembrane ion channels, transporters, and pumps, such as voltage gated sodium channels (including  $\text{Na}_v1.6$ ), as well as cell adhesion molecules and other scaffolding proteins (reviewed by Yoon et al.<sup>5</sup>). It is notable that, of the biallelic individuals, only two have variants which both affect the ANKRD, and these variants are missense variants. It is thus plausible that amorphic, biallelic disruption of these domains is not tolerated.

Predictive protein modeling of several of the missense variants found in or upstream of the ANKRD revealed conformational changes or altered surface electrostatic charges, which likely affect binding with one or more of the many interaction partners of the ANKRD, such as the motor protein KIF5. The ankyrin-G-KIF5 interaction is essential for the transport of the sodium channel  $\text{Na}_v1.2$  in the axon initial segments, and its disruption considerably reduces local  $\text{Na}_v1.2$  levels and may affect action potential firing.<sup>29</sup> Notably, both the p.(His112Tyr) variant in P13 and the p.(Asn227Lys) variant, which had a CADD score below the inclusion threshold (Tables S1 and S2), disturb the binding sites for KIF5. Only the p.(Asn227Lys) variant is predicted to alter protein structure, as it introduces a considerable narrowing of the angle between the N- and C-terminal moieties of the ANKRD, which likely alters protein function (Figure S2). Thus, although this variant has a low CADD score, it may have a pathogenic effect and necessitates functional studies. The only missense variant (p.(Pro1224Leu)) located in the highly conserved SBD, which links ankyrin-G to the cytoskeleton, is predicted to destabilize the local



structure, possibly affecting spectrin-binding. However, as this variant is *in trans* to the microdeletion (P3) encompassing six OMIM morbid genes, it is unclear whether the severe phenotype is due to either or both variants. 3D protein modeling with adequate quality of the giant exon and the serine-rich domain was impeded due to the lack of suitable templates, and thereby the effects of the missense variants located in these domains could not be predicted. However, future advances on resolving the structure of ankyrin-G (or other relevant templates) may enable prediction of the effect of the remaining missense variants.

In brief, this study confirms the importance of *ANK3* in the etiology of ID, developmental delay, behavioral issues (including ASD, ADHD/ADD, aggressivity/automutilation), hypotonia, sleep disturbances, and epilepsy. In general, individuals with biallelic variants had more clinical features compared to those with monoallelic variants. Detailed and standardized clinical phenotyping and correlation of genotype and phenotype will allow us to better understand the pathogenesis and identify early diagnostic and prognostic factors. This will be pivotal to improve prognostic accuracy and for the future identification of targeted treatment options. Functional analyses are needed to confirm the mechanism of action and assess severity of the allelic spectrum.

## AUTHOR CONTRIBUTIONS

**Conceptualization:** Zeynep Tümer, Elena Gardella, Rikke S. Møller; **Data Curation – genetic and clinical investigations:** Michael J. Bamshad, Tahsin Stefan Barakat, Meghan N. Bartos, Emilia K. Bijlsma, Francesco Brancati, Lucile Cejudo, Jessica X. Chong, Wendy K. Chung, Chiara De Luca, Sarah Joy Dean, Alena Egense, Himanshu Goel, Adam J. Guenzel Ulrike Hüffmeier, Eric Legius, Grazia M. S. Mancini, Tanguy Niclass, Marc Planes, Sylvia Redon, Karen Rouault, Rachel Schot, Sarah Schuhmann, Joseph J. Shen, Alice M. Tao, Miel Theunis, Isabelle Thiffault, Hilde Van Esch, Ingrid M. Wentzensen; **Data Analysis:** Francesca Furia, Amanda M. Levy, Paulino Gomez-Puertas, Iñigo Marcos-Alcalde, David Ros-Pardo, Elena Gardella, Zeynep Tümer; **Project Administration:** Francesca Furia, Amanda M. Levy, Elena Gardella, Zeynep Tümer; **Visualization:** Amanda M. Levy, Paulino Gomez-Puertas, Iñigo Marcos-Alcalde, David Ros-Pardo; **Writing – Original Draft Preparation:** Francesca Furia, Amanda M. Levy, Paulino Gomez-Puertas, Zeynep Tümer, Elena Gardella; **Writing – Review & Editing:** All authors; **Fine tuning and final editing of the manuscript:** Francesca Furia, Amanda M. Levy, Tahsin Stefan Barakat, Miel Theunis, Wendy K. Chung, Zeynep Tümer.

## AFFILIATIONS

<sup>1</sup>Department of Epilepsy Genetics and Personalized Treatment, The Danish Epilepsy Centre, Dianalund, Denmark

<sup>2</sup>Faculty of Health Science, University of Southern Denmark (SDU), Odense, Denmark

<sup>3</sup>Department of Clinical Genetics, Kennedy Center, Copenhagen University Hospital, Copenhagen, Denmark

<sup>4</sup>Center for Human Genetics, University Hospitals Leuven, Leuven, Belgium

<sup>5</sup>Department of Pediatrics, Division of Genetic Medicine, University of Washington, Seattle, Washington, USA

<sup>6</sup>Brotman-Baty Institute for Precision Medicine, University of Washington, Seattle, Washington, USA

<sup>7</sup>Department of Pediatrics, Division of Genetic Medicine, Seattle Children's Hospital, Seattle, Washington, USA

<sup>8</sup>Department of Genetics, The University of Alabama at Birmingham, Birmingham, Alabama, USA

<sup>9</sup>Department of Clinical Genetics, Leiden University Medical Centre, Leiden, The Netherlands

<sup>10</sup>Human Genetics, Department of Life, Health and Environmental Sciences, University of L'Aquila, L'Aquila, Italy

<sup>11</sup>Human Functional Genetics Laboratory, Istituto di Ricovero e Cura a Carattere Scientifico San Raffaele Roma, Rome, Italy

<sup>12</sup>CHU de Poitiers, Service de Génétique, Poitiers, France

<sup>13</sup>Division of Genomic Medicine, Department of Pediatrics, University of California Davis, Sacramento, California, USA

<sup>14</sup>General Genetics Service, Hunter Genetics, Waratah, New South Wales, Australia

<sup>15</sup>School of Medicine and Public Health, College of Health, Medicine and Wellbeing, University of Newcastle, Callaghan, New South Wales, Australia

<sup>16</sup>GeneDx Inc., Gaithersburg, Maryland, USA

<sup>17</sup>Institute of Human Genetics, Universitätsklinikum Erlangen, FAU Erlangen-Nürnberg, Erlangen, Germany

<sup>18</sup>Department of Clinical Genetics, Erasmus MC University Medical Center, Rotterdam, The Netherlands

<sup>19</sup>ENCORE Expertise Center for Neurodevelopmental Disorders, Erasmus MC University Medical Center, Rotterdam, The Netherlands

<sup>20</sup>Molecular Modeling Group, Centro de Biología Molecular Severo Ochoa (CBM, CSIC-UAM), Madrid, Spain

<sup>21</sup>Service de Génétique Clinique, CHRU de Brest, Brest, France

<sup>22</sup>Service de Génétique Médicale et Biologie de la Reproduction, CHU de Brest, Brest, France

<sup>23</sup>Université de Brest, INSERM, Etablissement Français du Sang, UMR 1078, Brest, France

<sup>24</sup>Discovery Unit, Department of Clinical Genetics, Erasmus MC University Medical Center, Rotterdam, The Netherlands

<sup>25</sup>Vagelos School of Physicians and Surgeons, Columbia University, New York, New York, USA

<sup>26</sup>Department of Pathology, Children's Mercy Kansas City, Kansas City, Missouri, USA

<sup>27</sup>Genomic Medicine Center, Children's Mercy Kansas City, Kansas City, Missouri, USA

<sup>28</sup>Laboratory for the Genetics of Cognition, KU Leuven, Leuven, Belgium

<sup>29</sup>Department of Pediatrics, Boston Children's Hospital, Boston, Massachusetts, USA

<sup>30</sup>Department of Pediatrics, Harvard Medical School, Boston, Massachusetts, USA

<sup>31</sup>Department of Neurophysiology, The Danish Epilepsy Centre, Dianalund, Denmark

<sup>32</sup>Department of Clinical Medicine, Faculty of Health and Medical Sciences, University of Copenhagen, Copenhagen, Denmark

## ACKNOWLEDGEMENTS

We thank all the included individuals and their families. Several of the authors of this publication are members of the European Reference Network on Rare Congenital Malformations and Rare Intellectual Disability ERN-ITHACA [EU Framework Partnership Agreement ID: 3HP-HP-FPA ERN-01-2016/739516], ERN-EpiCARE, ERN-GENTURIS, and/or ERN-RND. Michael J. Bamshad and Jessica X. Chong was supported by NHGRI grants U01 HG011744 and U24 HG011746 and acknowledges the University of Washington Center for Rare Disease Research (UW-CRDR) for their support in sequencing and analysis. Tahsin Stefan Barakat was supported by the Netherlands Organisation for Scientific Research (ZonMw Vidi, grant 09150172110002), an Erasmus MC Fellowship 2017, and Erasmus MC Human Disease Model Award 2018. Funding bodies did not have any influence on study design, results, and data interpretation or final manuscript. Francesco Brancati was supported by funding of the Italian Ministry of Health grants Ricerca corrente, LifeMap T3-AN-14 and the Italian Ministry of University and Research grants PRIN2022 and PRIN PNRR 2022. Wendy K. Chung was supported by P50HD109879. Paulino Gomez-Puertas, Iñigo Marcos-Alcalde, and David Ros-Pardo was supported by Spanish Government grants RTI2018-094434-B-I00, PID2021-126625OB-I00 (MCIN/AEI/10.13039/501100011033/FEDER,EU.2022) and DTS20-00024 (ISCIII) and gratefully recognizes the computational support of the Centro de Computación Científica CCC-UAM. Isabelle Thiffault was supported by generous gifts to Children's Mercy Research Institute and Genomic Answers for Kids program at Children's Mercy Kansas City.

## CONFLICT OF INTEREST STATEMENT

Ingrid M. Wentzensen and Adam J. Guenzel are employees of GeneDx, LLC. The remaining authors have no conflicts of interest to declare.

## DATA AVAILABILITY STATEMENT

The data analyzed in the current study are available in the Table S1.

## ORCID

Jessica X. Chong  <https://orcid.org/0000-0002-1616-2448>

David Ros-Pardo  <https://orcid.org/0000-0002-8934-8585>

Tahsin Stefan Barakat  <https://orcid.org/0000-0003-1231-1562>

Zeynep Tümer  <https://orcid.org/0000-0002-4777-5802>

## REFERENCES

- Smith KR, Penzes P. Ankyrins: roles in synaptic biology and pathology. *Mol Cell Neurosci*. 2018;91:91-139. doi:10.1016/j.mcn.2018.04.010
- Kordeli E, Lambert S, Bennett V. Ankyrin(G). A new ankyrin gene with neural-specific isoforms localized at the axonal initial segment and node of Ranvier. *J Biol Chem*. 1995;270(5):270-2359. doi:10.1074/jbc.270.5.2352
- Bennett V, Lorenzo DN. Spectrin- and Ankyrin-based membrane domains and the evolution of vertebrates. *Current Topics in Membranes*. Vol 72. Academic Press; 2013:1-73. doi:10.1016/B978-0-12-417027-8.00001-5
- Cunha SR, Mohler PJ. Ankyrin protein networks in membrane formation and stabilization. *J Cell Mol Med*. 2009;13(11-12):13. doi:10.1111/j.1582-4934.2009.00943.x
- Yoon S, Pignatelli NH, Penzes P. Roles and mechanisms of ankyrin-G in neuropsychiatric disorders. *Exp Mol Med*. 2022;54(7):867-877. doi:10.1038/s12276-022-00798-w
- Issa MY, Chechlac Z, Stanley V, et al. Molecular diagnosis in recessive pediatric neurogenetic disease can help reduce disease recurrence in families. *BMC Med Genet*. 2020;13(1):68. doi:10.1186/s12920-020-0714-1
- Kloth K, Denecke J, Hempel M, et al. First de novo ANK3 nonsense mutation in a boy with intellectual disability, speech impairment and autistic features. *Eur J Med Genet*. 2017;60(9):494-498. doi:10.1016/j.ejmg.2017.07.001
- Kloth K, Lozic B, Tagoe J, et al. ANK3 related neurodevelopmental disorders: expanding the spectrum of heterozygous loss-of-function variants. *Neurogenetics*. 2021;22(4):263-269. doi:10.1007/s10048-021-00655-4
- Yang R, Walder-Christensen KK, Lalani S, et al. Neurodevelopmental mutation of giant ankyrin-G disrupts a core mechanism for axon initial segment assembly. *Proc Natl Acad Sci USA*. 2019;116(39):19717-19726. doi:10.1073/pnas.1909989116
- Iqbal Z, Vandeweyer G, Van Der Voet M, et al. Homozygous and heterozygous disruptions of ANK3: At the crossroads of neurodevelopmental and psychiatric disorders. *Hum Mol Genet*. 2013;22(10):1960-1970. doi:10.1093/hmg/ddt043
- Younus M, Rasheed M, Lin Z, et al. Homozygous missense variant in the N-terminal region of ANK3 gene is associated with developmental delay, seizures, speech abnormality, and aggressive behavior. *Mol Syndromol*. 2023;14(1):11-20. doi:10.1159/000526381
- Fang X, Fee T, Davis J, Stolerman E, Caylor RC. Clinical case report: mosaic genetic variants in the ANK3 gene are associated with neurodevelopmental delays. *Mol Case Stud*. 2023;9(3):a006233. doi:10.1101/mcs.a006233
- Al-Dewik N, Mohd H, Al-Mureikhi M, et al. Clinical exome sequencing in 509 Middle Eastern families with suspected Mendelian diseases: the Qatari experience. *Am J Med Genet A*. 2019;179(6):927-935. doi:10.1002/ajmg.a.61126
- Bi C, Wu J, Jiang T, et al. Mutations of ANK3 identified by exome sequencing are associated with autism susceptibility. *Hum Mutat*. 2012;33(12):1635-1638. doi:10.1002/humu.22174
- Sanders SJ, Murtha MT, Gupta AR, et al. De novo mutations revealed by whole-exome sequencing are strongly associated with autism. *Nature*. 2012;485(7397):237-241. doi:10.1038/nature10945
- Zhu X, Petrovski S, Xie P, et al. Whole-exome sequencing in undiagnosed genetic diseases: interpreting 119 trios. *Genet Med*. 2015;17(10):774-781. doi:10.1038/gim.2014.191
- Hu H, Kahrizi K, Musante L, et al. Genetics of intellectual disability in consanguineous families. *Mol Psychiatry*. 2019;24(7):1027-1039. doi:10.1038/s41380-017-0012-2
- Allen AS, Berkovic SF, Cossette P, et al. De novo mutations in epileptic encephalopathies. *Nature*. 2013;501(7466):217-221. doi:10.1038/nature12439
- Panagiotakaki E, Tiziano FD, Mikati MA, et al. Exome sequencing of ATP1A3-negative cases of alternating hemiplegia of childhood reveals SCN2A as a novel causative gene. *Eur J Hum Genet*. 2023;32:224-231. doi:10.1038/s41431-023-01489-4

20. Philippakis AA, Azzariti DR, Beltran S, et al. The matchmaker exchange: a platform for rare disease gene discovery. *Hum Mutat.* 2015;36(10):915-921. doi:10.1002/humu.22858
21. Richards S, Aziz N, Bale S, et al. Standards and guidelines for the interpretation of sequence variants: a joint consensus recommendation of the American College of Medical Genetics and Genomics and the Association for Molecular Pathology. *Genet Med.* 2015;17:405-424. doi:10.1038/gim.2015.30
22. Wang C, Wei Z, Chen K, et al. Structural basis of diverse membrane target recognitions by ankyrins. *eLife.* 2014;3:e04353. doi:10.7554/eLife.04353
23. Wang C, Yu C, Ye F, Wei Z, Zhang M. Structure of the ZU5-ZU5-UPA-DD tandem of ankyrin-B reveals interaction surfaces necessary for ankyrin function. *Proc Natl Acad Sci USA.* 2012;109(13):4822-4827. doi:10.1073/pnas.1200613109
24. Ros-Pardo D, Gómez-Puertas P, Marcos-Alcalde Í. STAG2: computational analysis of missense variants involved in disease. *Int J Mol Sci.* 2024;25(2):1280. doi:10.3390/ijms25021280
25. Grosz BR, Golovchenko NB, Ellis M, et al. A de novo EGR2 variant, c.1232A > G p.Asp411Gly, causes severe early-onset Charcot-Marie-Tooth Neuropathy Type 3 (Dejerine-Sottas Neuropathy). *Sci Rep.* 2019;9(1):19336. doi:10.1038/s41598-019-55875-4
26. Wengert ER, Tronhjem CE, Wagnon JL, et al. Biallelic inherited SCN8A variants, a rare cause of SCN8A-related developmental and epileptic encephalopathy. *Epilepsia.* 2019;60(11):2277-2285. doi:10.1111/epi.16371
27. Strehlow V, Rieubland C, Gallati S, et al. Compound-heterozygous GRIN2A null variants associated with severe developmental and epileptic encephalopathy. *Epilepsia.* 2022;63(10):e132-e137. doi:10.1111/epi.17394
28. van der Werf IM, Van Dam D, Missault S, et al. Behavioural characterization of AnkyrinG deficient mice, a model for ANK3 related disorders. *Behav Brain Res.* 2017;328:218-226. doi:10.1016/j.bbr.2017.04.014
29. Barry J, Gu Y, Jukkola P, et al. Ankyrin-G directly binds to Kinesin-1 to transport voltage-gated Na<sup>+</sup> channels into axons. *Dev Cell.* 2014;28(2):117-131. doi:10.1016/j.devcel.2013.11.023

#### SUPPORTING INFORMATION

Additional supporting information can be found online in the Supporting Information section at the end of this article.

**How to cite this article:** Furia F, Levy AM, Theunis M, et al. The phenotypic and genotypic spectrum of individuals with mono- or biallelic ANK3 variants. *Clinical Genetics.* 2024;1-11. doi:10.1111/cge.14587

## Supplementary Methods

### Structural modeling and molecular dynamics simulation of the ANK3 missense variants

3D structures of the ANKRs, ZU5, UPA, and Death domains of wild-type (WT) ankyrin-G (UniprotKB id: Q12955) were modeled using the crystal structures of ankyrin-B repeats domain (PDB ID: 4RLV; <sup>1</sup>) and ZU5-ZU5-UPA-Death tandem (PDB ID: 4D8O; <sup>2</sup>) as templates. Due to unstructured sequences and the lack of a suitable template, it was not possible to generate a quality structural model for the rest of the protein domains. The SWISS-MODEL server (<http://swissmodel.expasy.org>) was used to build models of WT domains with structural quality within the range of those accepted for homology-based structures (Anolea/Gromos/QMEAN4). Protein models for ANK3 missense variants were generated using the WT structure as template. The initial positions of the side chains of the mutated residues were assigned using the Pymol Molecular Graphics System (<https://pymol.org/>).

Structures for wild-type and variant ANKR domains were subjected to 100 ns of unrestrained Molecular Dynamics (MD) simulation using the AMBER18 molecular dynamics package (<http://ambermd.org/>; University of California-San Francisco, CA), essentially as previously described <sup>3</sup>. In brief, 3D models were first solvated with a periodic cuboid pre-equilibrated solvent box using the LEaP module of AMBER, with 10 Å as the shortest distance between any atom in the protein domain and the periodic box boundaries. Free MD simulation was performed using the PMEMD program of AMBER18 and the ff14SB force field (<http://ambermd.org/>), applying the SHAKE algorithm, a time step of 2 femtoseconds (fs) and a non-bonded cut-off of 12Å. Systems were initially relaxed over 10,000 steps of energy minimization, using 1,000 steps of steepest descent minimization followed by 9,000 steps of conjugate-gradient minimization. Simulations were then started with a 20 picoseconds (ps) heating phase, raising the temperature from 0 to 300 K in 10 temperature change steps, after each of which velocities were reassigned. During minimization and heating, the C $\alpha$  trace dihedrals were restrained with a force constant of 500 kcal mol<sup>-1</sup> rad<sup>-2</sup> and gradually released in an equilibration phase in which the force constant was progressively reduced to 0 over 200 ps. After the equilibration phase, 100 ns of unrestricted MD simulation were obtained for the structures. MD trajectories were analyzed using VMD software <sup>4</sup>. Figures were generated using the Pymol Molecular Graphics System.

## REFERENCES

1. Wang C, Wei Z, Chen K, et al. Structural basis of diverse membrane target recognitions by ankyrins. *Elife*. 2014;3(November). doi:10.7554/eLife.04353
2. Wang C, Yu C, Ye F, Wei Z, Zhang M. Structure of the ZU5-ZU5-UPA-DD tandem of ankyrin-B reveals interaction surfaces necessary for ankyrin function. *Proc Natl Acad Sci U S A*. 2012;109(13). doi:10.1073/pnas.1200613109

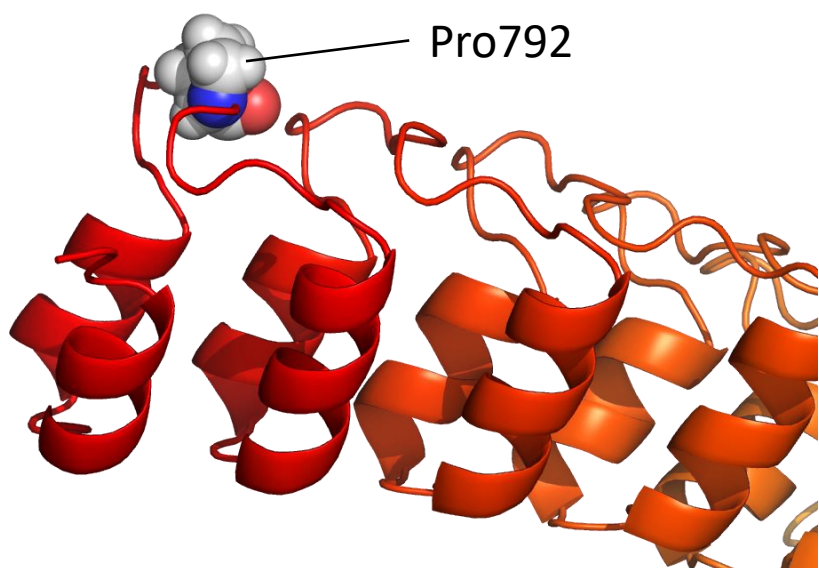
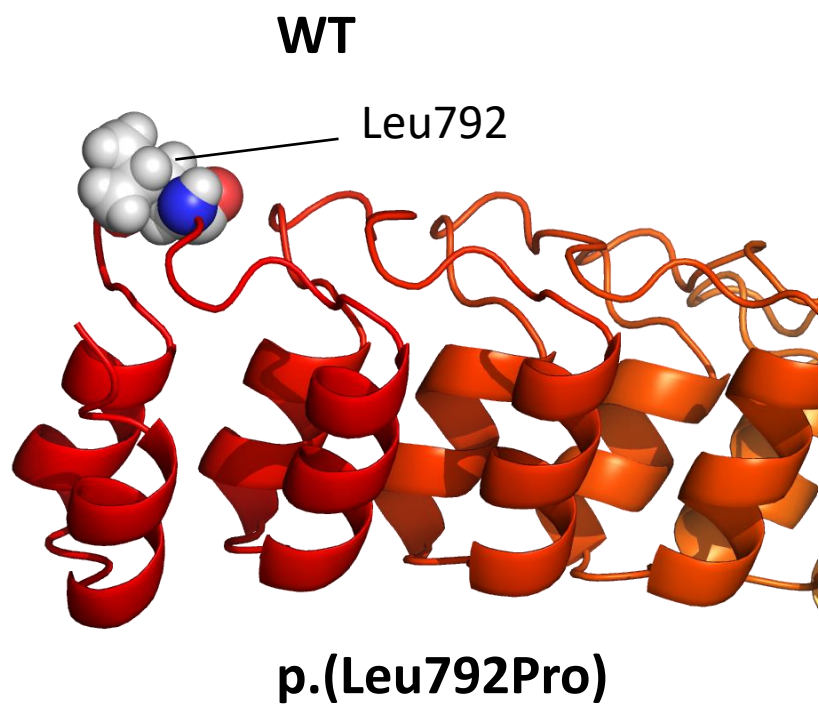
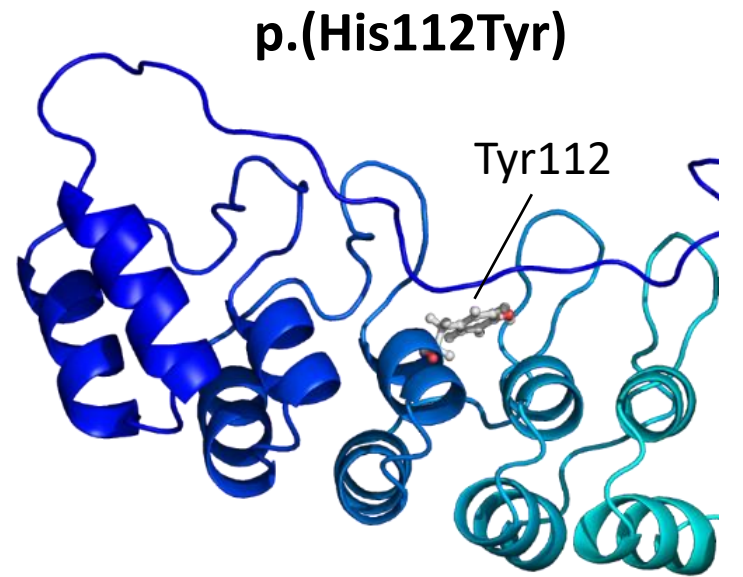
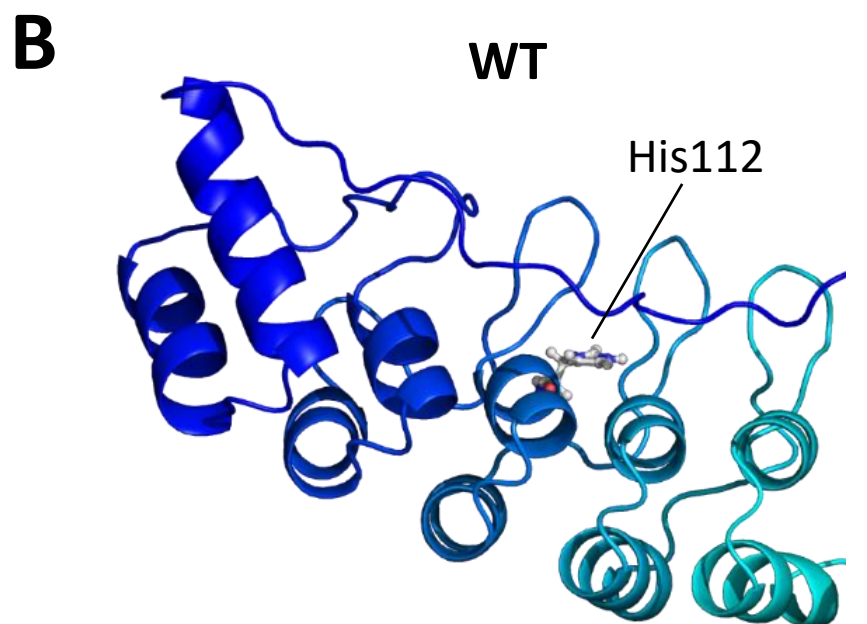
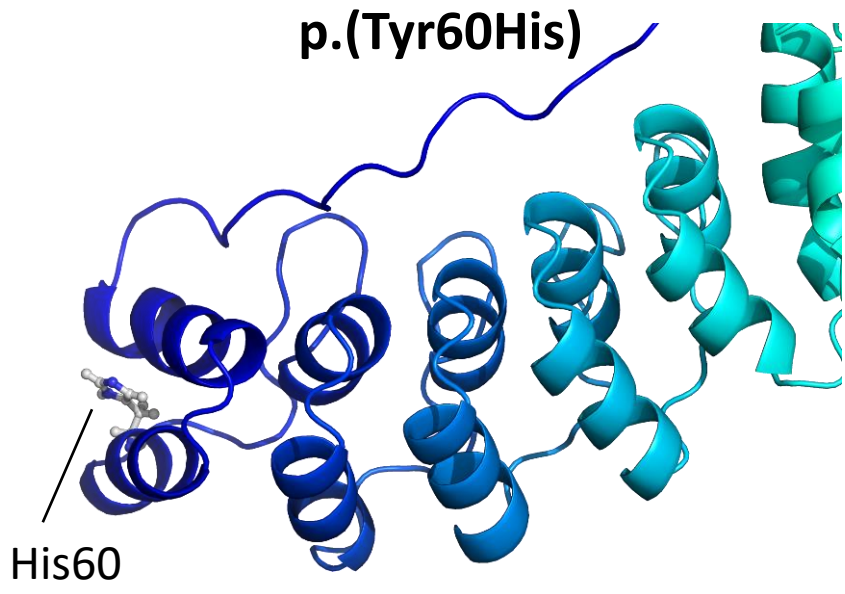
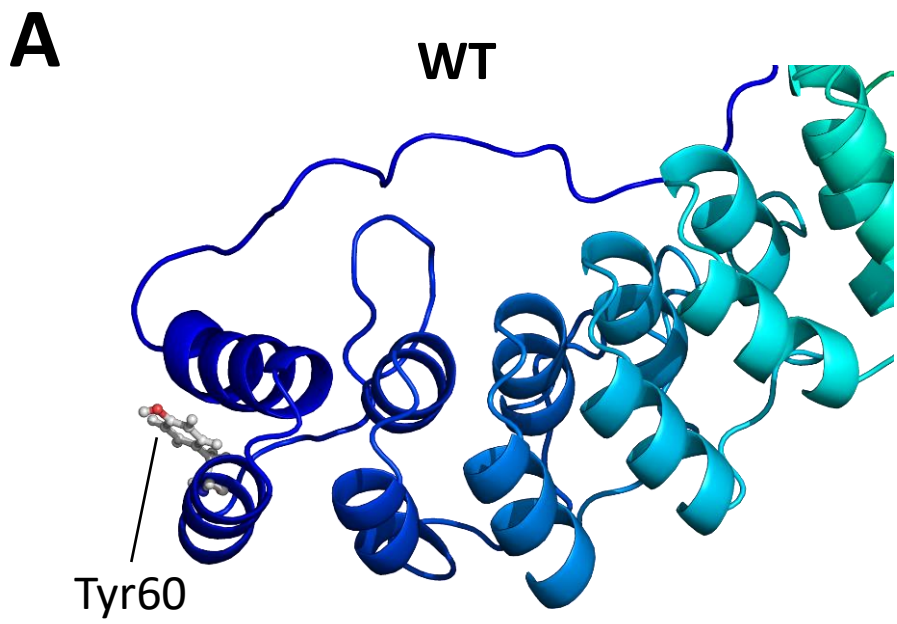
3. Ros-Pardo D, Gómez-Puertas P, Marcos-Alcalde Í. STAG2: Computational Analysis of Missense Variants Involved in Disease. *Int J Mol Sci.* 2024;25(2). doi:10.3390/ijms25021280
4. Humphrey W, Dalke A, Schulten K. VMD: Visual molecular dynamics. *Journal of Molecular Graphics.* 1996;14(1). doi:10.1016/0263-7855(96)00018-5

## Supplementary Figures

**Supplementary Figure S1.** Structural models of the ANK3 missense variants (A) p.(Tyr60His), (B) p.(His112Tyr), and (C) p.(Leu792Pro). Neither of the three variants are predicted to affect the structural or dynamic properties of the protein. WT, wild-type.

**Supplementary Figure S2.** Structural models of a ANK3 missense variants not fulfilling the CADD score inclusion criteria. p.(Asn227Lys) changes the structure of the ankyrin-repeat domain (ANKRD). WT, wild-type.





**WT**



**p.(Asn227Lys)**

